CrossMark

Investigation into the Anticancer Activity and Apoptosis Induction of Brevinin-2R and Brevinin-2R-Conjugated PLA–PEG–PLA Nanoparticles and Strong Cell Cycle Arrest in AGS, HepG2 and KYSE-30 Cell Lines

Robab Hassanvand Jamadi[1] · Asadollah Asadi[1] · Hashem Yaghoubi[2] · Fariba Goudarzi[1]

Abstract
Our study aims to establish a biocompatible nanostructure for the improved delivery of anticancer peptide, Brevinin-2R, to treat human gastric adenocarcinoma (AGS), human liver hepatocellular carcinoma (HepG2) and human squamous cell carcinoma (KYSE-30) cells. Poly(ʟ-lactide)–poly(ethylene glycol)–poly(ʟ-lactide) (PLA–PEG–PLA) nanoparticles were synthesized, obtained by a solvent evaporation method and characterized using scanning electron microscopy (SEM), FTIR and DLS; chemically-synthesized Brevinin-2R was encapsulated in micelles. In vitro release and cell uptake assay were conducted before cytotoxicity tests. Cell cycle analysis and apoptosis study were performed through flow cytometry and Annexin-V-FlOUS cell staining. PLA–PEG–PLA nanoparticles showed a narrow-size distribution with a zeta potential of −26.63 and a high cell internalization. Brevinin-2R-conjugated nanoparticles were spherical in shape with an increased surface charge of −21.90. For the first time, viability tests showed that Brevinin-2R-conjugated nanoparticles were more efficient than Brevinin-2R against cancer cells causing higher rates of cell cycle arrest and apoptosis induction. Our new findings demonstrate the potential of PLA–PEG–PLA nanoparticles to boost the anticancer effect and improve the delivery of Brevinin-2R. The study of Brevinin-2R-loaded nanoparticles indicated noticeable results in terms of novel cancer therapy. PLA–PEG–PLA nanoparticles can act as a biocompatible delivery platform to take the advantage of Brevinin-2R toward cancer cells. This is a novel study as the Brevinin-2R-conjugated nanoparticles and applied approaches have not been already reported.

Keywords Apoptosis induction · Brevinin-2R-conjugated nanoparticle · Cell cycle arrest · Cell internalization · Drug loading · Enhanced anticancer efficiency

Introduction

Although progress in diagnosis and therapy has noticeably decreased the mortality of cancer, it is still a pervasive problem (Perez-Tomas 2006). Cancer therapy using custom chemical drugs and surgery is accompanied by toxicity and severe side effects on normal tissues and cells (Hami et al. 2014a, b; Kakde et al. 2011). Brevinin-2R, with the amino acid sequence of KLKNFAKGVAQSLLNKASCKLSGQC (Ghodsi-Moghadam and Asoodeh 2018), is a synthesized antimicrobial peptide that belongs to the Brevinin-2 family (Ghavami et al. 2008). With 25 amino acid and a net charge of +5, in spite of a majority of Brevinins, it shows a negligible hemolytic action toward red blood cells (Ghavami et al. 2008). This peptide shows antimicrobial activity against gram-positive and gram-negative bacteria (Ghodsi-Moghadam and Asoodeh 2018). Added to anti-bacterial activity on reference strains of bacteria, this water-soluble peptide has dramatically exhibited an anti-proliferating effect on a broad spectrum of cancer cell lines (Asoodeh et al. 2013; Ghavami et al. 2008), inhibiting the growth of Jurkat, BJAB, HT29/219, SW742 and some other cell lines (Ghavami et al. 2008; Homayouni-Tabrizi et al. 2015; Mehrnejad et al.

✉ Robab Hassanvand Jamadi
   robab.hasanvand@yahoo.com

1   Department of Biology, Faculty of Sciences, University of Mohaghegh Ardabili, Ardabil, Iran

2   Department of Biology, Ardabil Branch, Islamic Azad University, Ardabil, Iran

2008).Thanks to its negligible hemolytic activity, Brevinin-2R can be considered as a promising therapeutic agent (Ghodsi-Moghadam and Asoodeh 2018).

Drug delivery systems such as micelle-like nanoparticles (Chan et al. 2009; Licciardi et al. 2010) can reduce side effects and dosages by improving targeted drug delivery and increasing antitumor efficacy (Li et al. 2008; Venkatraman et al. 2005). Polymeric micelles are nano-sized carriers (Yokoyama 2011) with amphiphilic block copolymers, consisting of PLA–PEG block copolymers (Jelonek et al. 2016) that are usually prepared by self-assembly (Woraphatphadung et al. 2018). With a hydrophobic inner core and hydrophilic corona, PLA–PEG–PLA nanoparticles can encapsulate drugs. Also, some other advantageous properties of these nanoparticles include high solubility, high stability, superior biocompatibility, biodegradability (He et al. 2007), controlled drug release, prolonged circulation in the bloodstream, high drug loading, well suited size (20–200 nm), selective accumulation in tumor sites and escaping the reticuloendothelial system (RES), renal exclusion, tumor targeting by improved permeability, etc. (Chau et al. 2006; He et al. 2007; Hrubý et al. 2005; Kataoka et al. 2001; Massodi et al. 2010; Phan et al. 2016; Venkatraman et al. 2005). Due to these properties, PLA–PEG–PLA nanoparticles have been considered as effective delivery systems. Thus, they can improve the antitumor efficacy and reduce toxicity (Ghavami et al. 2008) that illustrate a high capacity to be developed in drug delivery (Duda et al. 1998; Mehrnejad et al. 2008; Woraphatphadung et al. 2018; Xiao et al. 2010; Zhao et al. 2012). The PLA and PEG copolymerization can raise loading efficiency (LE), decrease the burst effect, and increase sustained drug release that is significantly related to the controlled micelles' degradation (Dell'Erba et al. 2001; Xiao et al. 2010). Given the expectation of only 10–15% of tumor cells being in the mitotic stage of the cell cycle at any time, the prolonged drug release is highly beneficial (Wolinsky et al. 2012).

Gastric cancer is the fourth most common malignant neoplasm and the second leading cause of cancer-related mortality worldwide (Li and Gao 2018). Despite decreasing mortality related to gastric cancer, about 700,000 confirmed deaths have been reported around the globe, annually (Jemal et al. 2011). Liver cancer is the third main cause of cancer-related deaths all over the world, being responsible for about 9.1% of total deaths in 2012 (Nakagawa et al. 2018). Esophageal cancer is the 8th most common cancer in the world and the 6th cause of cancer deaths. The esophageal squamous cell carcinoma is the dominant histological subtype of esophageal cancer globally, followed by adenocarcinoma (Allum et al. 2018; Middleton et al. 2018).

The aim of this study was to synthesize Brevinin-2R and Brevinin-2R-conjugated polymeric micelles, in vitro evaluation of release behavior in phosphate buffer solution (pH 7.4), cellular uptake, investigation into inhibitory effects of Brevinin-2R and Brevinin-2R-conjugated nanoparticles on AGS, HepG2 and KYSE-30 cell lines, cell cycle arrest and apoptosis induction. PLA–PEG–PLA micelles, prepared by a solvent evaporation method, were characterized for particle size distribution, shape, structure, average size, biocompatibility and cell internalization through scanning electron microscopy (SEM), FTIR, DLS, hemolysis assay, confocal laser scanning microscopy; the results revealed that PLA–PEG–PLA triblock copolymer and Brevinin-2R were successfully synthesized. PLA–PEG–PLA nanoparticles were localized into selected cancer cells. For the first time, we conducted the study on the in vitro cytotoxicity of synthesized Brevinin-2R and Brevinin-2R-conjugated micelles against the above mentioned cell lines using the 3-(4,5-dimethylthiaol-2-yl)-2,5-diphenyltetrazolium bromide (MTT) and neutral red (NR) uptake assays. Results revealed severe cytotoxic effect of Brevinin-2R-conjugated nanoparticles compared to that of Brevinin-2R. Our fresh evidence also elucidated the cell cycle arrest and apoptosis induction in treated cancer cells.

Materials and Methods

Materials

The AGS, HepG2, KYSE-30 and human normal fibroblast of gingiva (HGF1-PI1) cell lines were purchased from the Pasteur institute, Iran; cell culture media and antibiotics were purchased from GIBCO; toluene, acetone, methanol, ethanol, acetic acid, dimethyl sulfoxide (DMSO), phosphate buffered saline (PBS) (pH 7.4), MTT and NR dye were prepared from Merck (Darmstadt, Germany); trypsin–EDTA, lactic acid (LA), poly(ethylene glycol) (PEG) with a molecular weight of 2000, *N,N*-dimethyl formamide (DMF) and fluorescein isothiocyanate (FITC) were prepared from Sigma-Aldrich (USA). Distilled water was applied for all experiments. The other chemicals and solvents were of analytical grade and employed without further purification.
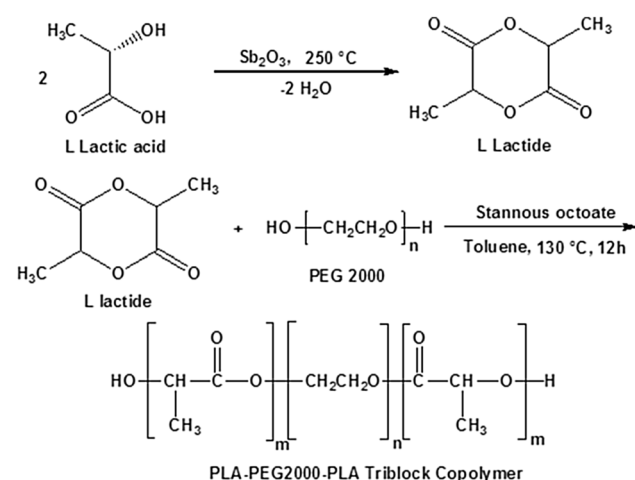
Peptide Synthesis

Brevinin-2R was designed and manually synthesized through solid phase strategies, using standard Fmoc chemistry, as previously described (Amaral et al. 2012; Hilpert et al. 2008). Purification of peptide was performed on a C18 analytical reverse phase high pressure chromatography (RP-HPLC) column (Pharmacia Biotech, US) with a linear gradient of acetonitrile in 0.1% TFA. Purified peptides were then characterized through a mass spectrometer (LTQ orbitrap, Thermo Electra, San Jose, CA) and C8 semi preparative RP-HPLC.

Synthesis of PLA–PEG–PLA Triblock Copolymer

Ring-opening polymerization of the lactide was employed for synthesizing the 44.5%PLA–11%PEG$_{2000}$–44.5%PLA tri-block copolymer in the presence of polyethylene glycol (PEG) under optimized conditions. Briefly, L-lactide was prepared from L-lactic acid, using antimony trioxide (Sb$_2$O$_3$) as a catalyst. In order to eliminate the residual impurities in the monomer, the synthesized L-lactide was re-crystallized from ethyl acetate and vacuum dried at 40 °C, overnight (High Vacuum Evaporation Systems, Model: ETS-160, EDS-160, High Vacuum Technology Center-ACECR, Sharif Branch, Iran). Afterward, 16 g of the vacuum-dried lactide and 3 g of PEG$_{2000}$ were dissolved in anhydrous toluene with the protection of nitrogen. 200 mg stannous octoate (Sn(Oct)$_2$) was then added into the reaction flask as a catalyst [0.15% (w/w), in toluene solution] (Fig. 1). Polymerization reaction was carried out at 130 °C under inert gas atmosphere. After 12 h, solvent was evaporated and the dried copolymer was repeatedly purified by dissolution in dichloromethane and crystallization from cold ethanol, and the obtained mixture was centrifuged, supernatant was then removed and the pellet vacuum was dried at 45 °C for 48 h.

Size and Zeta Potential of Nanoparticles

The average particle size distribution and zeta potential of blank micelles, as well as Brevinin-2R-conjugated micelles were measured using dynamic light scattering, through a 90 PLUS Zeta potential analyzer (Brookhaven Instruments Cooperation. New York, USA) at 25 °C with a scattering angle of 90°. The measurement was conducted using a clear disposable sizing cuvette which eventuate a hydrodynamic diameter for the particles. All results were the average of three different test runs.

Biocompatibility of Nanoparticles

Freshly isolated human blood from a healthy donor was washed three times with the same volume of PBS (pH 7.4), centrifuged at 150×g for 5 min, and resuspended in PBS to obtain a final concentration at 4% (v/v). Then various concentrations of copolymer were incubated with the washed RBCs at 37 °C for 30 min. Red blood cells in PBS and 0.2% Triton X-100 were considered as negative and positive controls, respectively; after centrifugation (10 min, 900×g), the supernatants were carefully transferred to a micro plate and the release of hemoglobin was monitored at 540 nm through micro-plate reader. HC$_{50}$ value was taken as the mean concentration causing 50% hemolysis.

Preparation of Brevinin-2R-Loaded Polymeric Micelles

Brevinin-2R-loading in PLA–PEG–PLA micelles was conducted by a solvent evaporation method. In brief, an optimized amount of Brevinin-2R was dissolved in distilled water (1 mg/ml). Polymeric nanoparticles were dissolved in acetone (1% W/W) (10 mg/ml). Afterward, 1 ml of peptide solution was added drop-wise to concentration of 10 ml of PLA–PEG–PLA solution in acetone under magnetic stirring for 4 h at room temperature. Acetone was then evaporated and the mixture was centrifuged at 3000 rpm for 10 min to eliminate unloaded Brevinin-2R. The resulting pellet, included stabilized Brevinin-2R-conjugated copolymeric micelles, dispersed for following studies. The concentration of free Brevinin-2R in supernatant was measured through Bradford protein assay (Davies et al. 1997; Zohri et al. 2010). The samples were evaluated and the LE was determined through the equation below:

$$LE\ (\%) = \frac{(Brevinin-2R_{total}) - (Brevinin-2R_{supernatant})}{Brevinin-2R_{total}} \times 100$$

Particle Morphology

The morphology and structural characteristics of nanoparticles and Brevinin-2R-conjugated micelles were assessed using SEM (LEO 1430 VP, UK) equipped with an Electron Microscope Camera (Fanavari Khala Kahroba Co., Iran). Diluted solutions of micelles and conjugates were placed onto a glass slide and dried in vacuum. The samples were mounted on metal stub plating and coated under the vacuum prior to observation.

Fig. 1 Synthesis of L-lactide and PLA–PEG$_{2000}$–PLA tri-block copolymer

FTIR Spectroscopy

The FTIR transmission spectra of PLA–PEG–PLA copolymer and Brevinin-2R-loaded copolymer were collected on a Perkin Elmer spectrum RXI spectrometer (Waltham, MA, USA) using the KBr pellets in the wave number region of 400–4000 cm^{-1} under a resolution of 4 cm^{-1} and with a scanning speed of 2 mm s^{-1} at 25 °C. FTIR was applied to identify the functional groups involved in the formation of the nanoparticles and investigate the interaction between the PLA–PEG–PLA copolymer and Brevinin-2R in conjugates.

In Vitro Release Study

In vitro release study of Brevinin-2R-loaded micelles was conducted using the dialysis technique. 5 ml of suspension was enclosed in a pre-soaked dialysis bag (MW cutoff: 12 kDa) immersed in a diffusion cell containing 50 ml PBS (pH 7.4) as a release medium, which was then incubated at 37 °C under constant shaking to avoid an unstirred water layer formation at the membrane/release medium interface. At regular time intervals, 1 ml samples were withdrawn for analysis of the Brevinin-2R concentration and the release medium was then replaced with an equal volume of fresh PBS to maintain a sink condition. The concentration of released Brevinin-2R was detected by UV/Vis spectrophotometer (Teif sanj pishro pajohesh, Iran) at 520 nm (11). The release data have been shown as the amounts of released drug relative to the total drug content in the conjugates. All experiments were performed in triplicate.

Cell Culture

The AGS, KYSE-30 and HepG2 and HGF1-PI1 cell lines were cultured in RPMI-1640 and supplemented with 10% fetal bovine serum (FBS), 100 unit/ml penicillin and 100 μg/ml streptomycin. After incubation at 37 °C in a water saturated atmosphere of 5% CO_2, the cells were plated in micro plates (around 1×10^4 cells per well) and went through an overnight incubation.

Qualitative Cellular Uptake Study

In order to visualize cell internalization of copolymeric micelles, AGS, KYSE-30 and HepG2 cancer cells were seeded at a density of 4×10^5 cells/well on coverslips in 6-well plates for fluorescence microscopy until they formed a monolayer. The medium was then eliminated and cells were incubated with the FITC-conjugated micelles (weight ratio 1:1). After 4 h of incubation, the cells were washed three times with cold PBS and fixed with 4% paraformaldehyde in PBS for 15 min at room temperature and then rinsed twice with fresh PBS. The fixed cells were subjected to a confocal laser scanning microscope (IX 71, Olympus, Japan) equipped with a digital camera (DP 71, OLYMPUS). Free FITC (1 μM) was used as the control.

Cell Viability Assay

MTT Assay

To determine cytotoxic efficacy of nanoparticles, Brevinin-2R and Brevinin-2R-loaded PLA–PEG–PLA micelles in vitro, AGS, HepG2, KYSE-30 and HGF1-PI cells were seeded in 96-well plates (5×10^3 cells/well), 24 h prior to the cytotoxicity test. Then, various concentrations of nanoparticles, Brevinin-2R and micelles conjugates in RPMI-1640 medium were added to the wells and further incubated for 24, 48, and 72 h. Then, 20 μl MTT (5 mg/ml) was added to wells and cells were incubated for 4 h. After removing the MTT solution, the cells were incubated with 150 μl DMSO for 10 min to dissolve the formazan crystals formed only by living cells. Thereafter, the absorbance of wells was determined using a microplate reader (Synergy HT, BioTek) at 540 nm. The IC$_{50}$ values were calculated as the drug concentrations that inhibit cell growth by 50%.

Neutral Red Uptake Assay

The cytotoxicity of nanoparticles, Brevinin-2R and Brevinin-2R-loaded PLA–PEG–PLA micelles against AGS, HepG2, KYSE-30 and HGF1-PI1 cell lines were determined with NR assay. Briefly, cells were plated into a 96-well plate (5×10^3 cells/well). After 24 h, cells were incubated for 24, 48, and 72 h with different concentrations of nanoparticles, Brevinin-2R and Brevinin-2R-conjugated micelles. After incubation time points, the medium was removed and a medium containing NR (20 ml of 0.05% NR solution) was added to wells and cells were then incubated for 3 h. After removing the NR solution, the cells were rinsed with PBS (37 °C) and 150 μl fixative solution (50% ethanol 96%, 49% deionized water and 1% glacial acetic acid) was added to wells; after 5 min of gentle shaking, the absorbance was detected with a micro plate reader (Synergy HT, BioTek) at 540 nm.

Cell Cycle Arrest Analysis

Cell cycle distribution and DNA content of treated cells with Brevinin-2R and Brevinin-2R-loaded nanoparticles were evaluated through flow cytometry. AGS, HepG2 and KYSE-30 cells were treated with Brevinin-2R and Brevinin-2R-loaded nanoparticles for 48 h and then rinsed with PBS. After fixing with ice cold ethanol for 2 h, cells were again rinsed and after adding propidium-iodide staining solution (sigma) incubated for 40 min; afterward, cells were

evaluated by the flow cytometer (Partec, Germany) and then Cell cycle profiles were analyzed using Flomax Software (Partec, Germany).

Apoptosis Study by Annexin-V-FLOUS-PI

AGS, KYSE-30 and HepG2 cells, treated with Brevinin-2R and Brevinin-2R-loaded nanoparticles (48 h), were rinsed with PBS and went through 20 min incubation with Annexin-inV FLOUS (20 ml) and PI (20 ml) (Roche) at 25 °C. After staining, cells were rinsed and suspended into the incubation buffer and apoptotic cells were studied through flow cytometry.

Statistical Analysis

All experiments were conducted repeatedly at least three times in triplicate. Data were graphed and analyzed by GraphPad Prism Software 7.03 using one-way analysis of variance (ANOVA) and the Student's *t* test and expressed as the mean ± SD; $P < 0.05$ was considered statistically significant.

Result and Discussion

Synthesis of Peptide

In order to mass confirmation, the synthesized peptide was purified through HPLC (Fig. 2A) and then subjected to the mass spectrometer. Mass analysis proved the expectation and validate the mass ion of m/z 2634.63 for Brevinin-2R (Fig. 2B).

Dynamic Light Scattering and Zeta Potential

DLS measurements illustrated the mean hydrodynamic diameter of 48 nm and 100 nm for PLA–PEG$_{2000}$–PLA nanoparticles and Brevinin-2R-conjugated nanoparticles, respectively. Also, zeta potential measurement displayed the surface charge of − 26.63 and − 21.90 mV for blank nanoparticles and Brevinin-2R-loaded nanoparticles, respectively. The smaller surface charge of blank micelles may be due to the arrangement of PEG on the outer layer of nanoparticles.

Particle Size Distribution and Morphology of Nanoparticles

The obtained micrographs expose the formation of spherical micelles as smooth and discrete spots with a size distribution of 40–80 nm for nanoparticles (Fig. 3A) and 70–150 nm for Brevinin-2R-loaded nanoparticles (Fig. 3B); hence the mean diameters of the Brevinin-2R-loaded micelles were larger

than those of corresponding blank micelles. The enlargement of the particle size because of Brevinin-2R incorporation into the hydrophobic core might be attributed to interactions between Brevinin-2R and copolymer, leading to the variation in size. As a macromolecule, Brevinin-2R could boost the diameter, however, Brevinin-2R-loaded nanoparticles can easily enter tumor capillaries with pore cutoff size ranging 200 nm to 1.2 µm. The conjugates prepared in this study may also avoid the mononuclear phagocytic system (MPS) and culminate in prolonged blood circulation (Hami et al. 2014a; Hobbs et al. 1998; Phan et al. 2016).

FTIR Analysis

The polymerization of PLA–PEG$_{2000}$–PLA triblock copolymer and Brevinin-2R loading on micelles were characterized by FTIR spectroscopy. To display the most important bands of absorption, the second order derivatives of FTIR spectra were determined using the spectrometer software OPUS (Fig. 4). The spectrum analysis of triblock PLA–PEG–PLA copolymer displayed characteristic vibrational modes including stretching frequencies for asymmetric and symmetric motions; the band at 2899.25 cm^{-1} corresponded to the C–H stretching vibration of –CH$_3$ groups of the PEG. The characteristic sharp and intense bands at 1760.68 and 1122.58 cm^{-1} confirm the presence of the carboxylic ester (C=O in PLA) and ether (C–O–C from PEG block) groups. The peak at 1456.79 cm^{-1} is attributed to a C–H bond of the methyl group. Bending frequencies for the –CH$_3$ symmetric have been identified at 1356.13 cm^{-1}. Band of C–C–O stretching of PEG chains appears around 952.98 and 838.85 cm^{-1}. The FTIR spectrum of PLA–PEG–PLA copolymer detected the presence of two constituent blocks in polymer, indicating the ring opening polymerization of lactide and formation of a PLA–PEG–PLA triblock copolymer (Fig. 4A) (Asadi et al. 2011; Zhao et al. 2012).

FTIR spectrum of Brevinin-2R-loaded nanoparticles (Fig. 4B), characterizing the potential interactions between Brevinin-2R and nanoparticles, is accompanied by slight shifts in absorption bands of amino and carboxylic groups, and amide bonds due to the possible interaction of a carboxyl group of the polymer with the amino group of Brevinin-2R; this evidence can be taken into account as an indication for the presence of Brevinin-2R into the nanoparticles.

The representative intensity at 3542.55 cm^{-1}, related to N–H and O–H stretching vibrations for the Brevinin-2R-loaded nanoparticles, is due to the incorporation of Brevinin-2R into the nanoparticles through probability of physicochemical interactions. The peak at 3158.02 cm^{-1} is thought to be the N–H bending vibration of amide A and the peak at 2559.29 is ascribed to CH$_2$ stretching vibration. The absorption band at 1094.46 cm^{-1} is assigned to the C–O stretching in the secondary hydroxyl group (characteristic
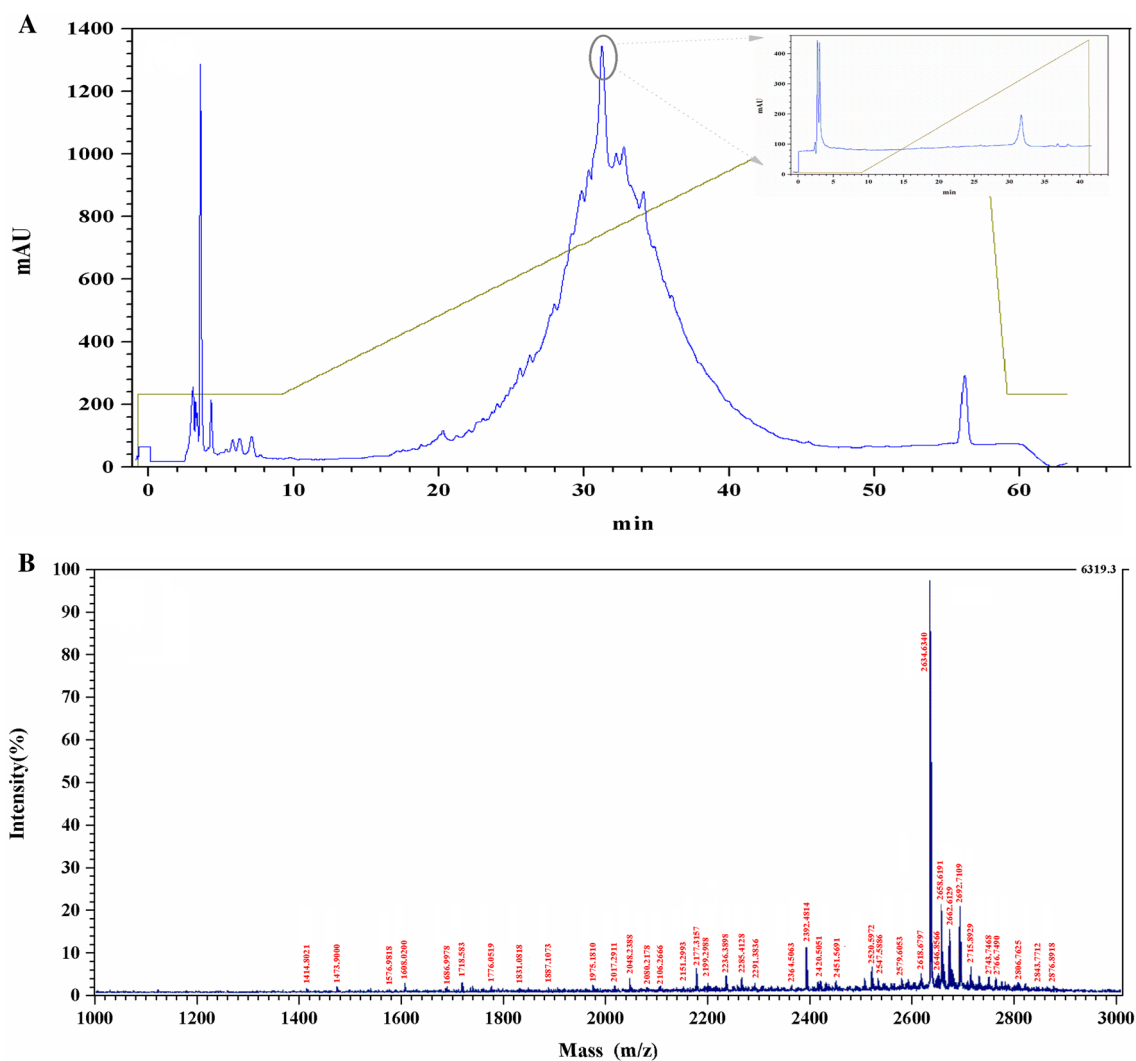
Fig. 2 A Chromatography of crude peptide in C18 analytical RP-HPLC column. Only encircled fraction was further purified by C8 reverse-phase semi-preparative columns. The inset depicts the chromatogram of the pure Brevinin-2R gained from analytical C8 reverse-phase column. **B** MALDI-TOF mass spectral data confirmed the expected molecular mass for Brevinin-2R. The spectrum was collected in a scan range of 999–3012 m/z

Fig. 3 SEM imaging by 300 nm order of magnitude for: nanoparticles (**A**) and Brevinin-2R-conjugated PLA–PEG–PLA micelles (**B**)
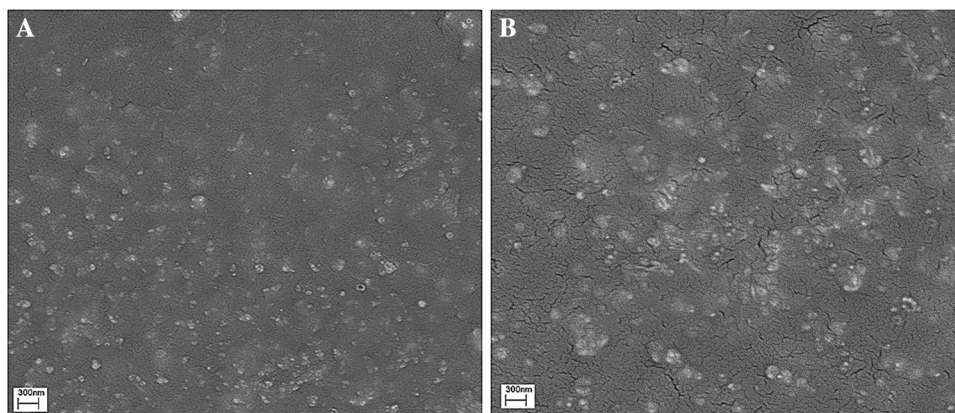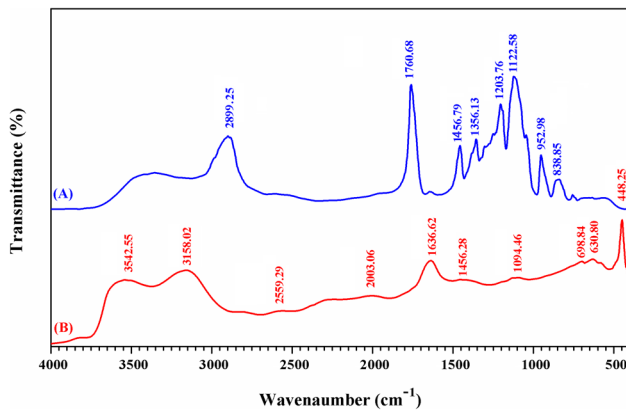
Fig. 4 FT-IR spectra for PLA–PEG–PLA polymeric nanoparticles (**A**) and Brevinin-2R-loaded PLA–PEG–PLA (**B**) in the region of 4000–400 cm^{-1}

peak of –CH–OH). The amide I band is the most sensitive and intense absorption band in the protein secondary structural components. Its frequency is found in 1636.62 cm^{-1}; it is associated with the C=O stretching vibrations of the peptide bond (amide I) and is directly related to backbone conformation and hydrogen bonding pattern. The peak at 1456.28 cm^{-1} is attributed to peptide side-chain –COO and also polymer carboxyl that are overlapped. The peaks at 698.84 and 630.80 are attributed to O=C–N and NH

bending (amide IV and amide V). Accordingly, there is a relocation for amide I band on account of some intermolecular and electrostatic interactions between Brevinin-2R and PLA–PEG–PLA. The peak at 3542.55 is ascribed to the stretching vibration of –OH and –NH; FTIR data analysis demonstrated efficient incorporation of Brevinin-2R in the PLA–PEG–PLA micelles.

Biocompatibility Assay

The hemolytic activity of PLA–PEG–PLA copolymer against human red blood cells was considered as a criterion for toxicity to mammalian cells. According to our data, at a concentration range of 2.5–80 mg/ml, the hemolytic activity of PLA–PEG–PLA polymeric nanoparticle toward human erythrocytes being measured at less than 5% (Fig. 5), indicates low hemolytic activity (P < 0.05), displaying its qualification as a proper biocompatible drug delivery system.

Cell Uptake and Internalization

Fluorescence microscopy was utilized to visualize the effect of PLA–PEG–PLA co-polymeric micelles on the cellular uptake by the AGS, KYSE-30 and HepG2 cells. Taking free FITC as a negative control, the fluorescence of FITC-labeled co-polymeric micelles provided evidence for internalization of polymeric micelles; cytoplasmic distribution

Fig. 5 **A** Hemolytic activity diagram for PLA–PEG–PLA polymeric nanoparticles against human erythrocytes. **B** Hemolysis test for PLA–PEG–PLA polymeric nanoparticles: (A) positive control; (B) negative control; (C) 2.5 mg/ml; (D) 5 mg/ml; (E) 10 mg/ml; (F) 20 mg/ml; (G) 40 mg/ml; (H) 80 mg/ml
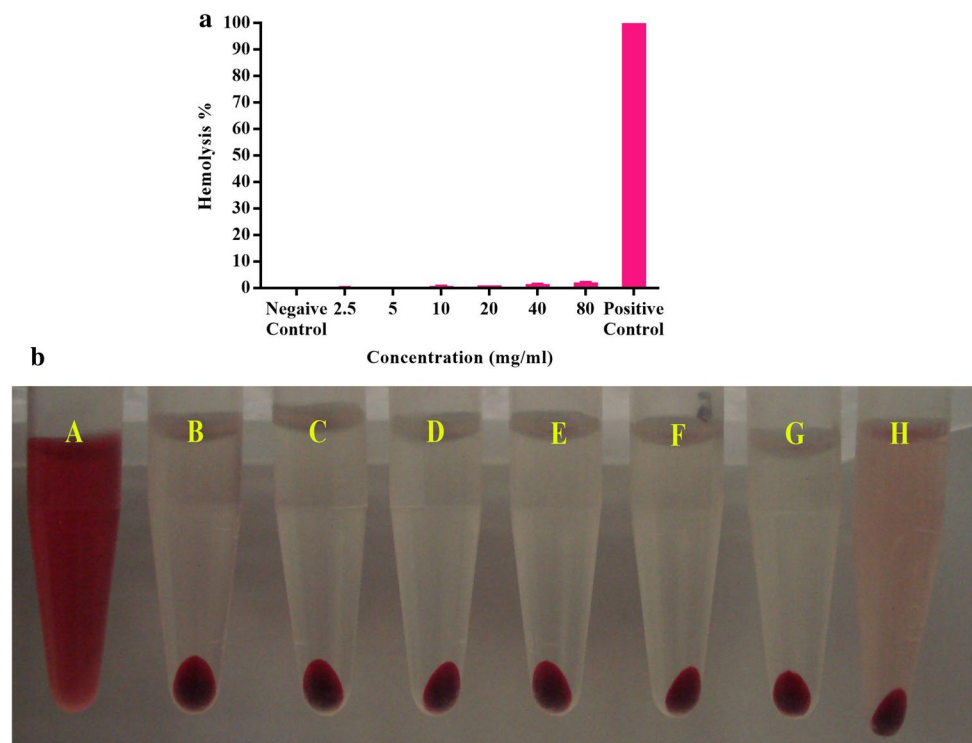
Fig. 6 **A** Confocal microscopy images of PLA–PEG–PLA co-polymeric nano micelles uptake by cancer cells after 4 h incubation with FITC-labeled polymer vs. control FITC treated cells. (b) AGS cell treated with FITC-labeled polymer, (a) control; (d) KYSE-30 cell treated with FITC-labeled polymer, (c) control; (f) HepG2 cell treated with FITC-labeled polymer, (e) control. **B** In vitro (PBS pH 7.4, 37 °C) release profile of Brevinin-2R from the PLA–PEG–PLA nanoparticles; each point represents mean ± SD for three samples and error bars represent the SD (n = 3)
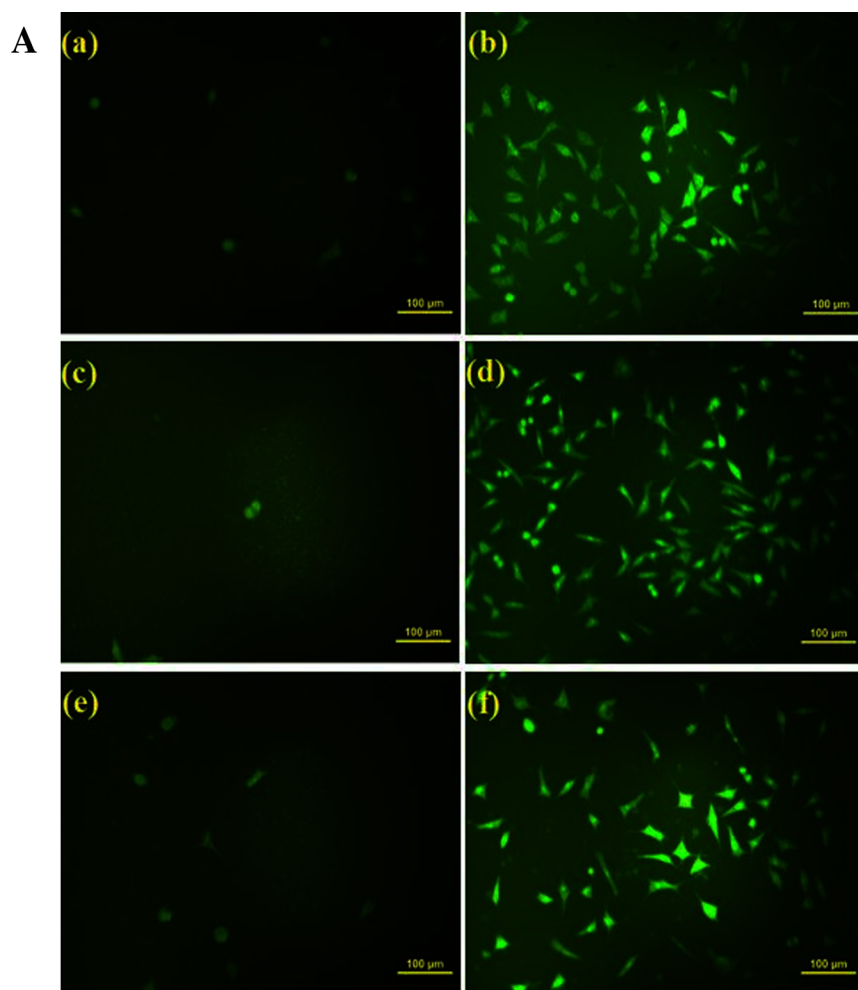
of FITC-labeled micelles was indicated through strong cell-associated green fluorescence (Fig. 6A). As expected, there was no fluorescence in samples with free FITC (Fig. 6A—a, c, e). The internalization of PLA–PEG–PLA micelles into AGS, KYSE-30 and HepG2 cells has plausibly come about by endocytosis. Penetrating plasma membrane and translocating into the cytoplasm of the cancer cells highlighted that the FITC-labeled nanoparticles did not lead to disruption of cell membrane integrity (Fig. 6A—b, d, f), indicating the feasibility of triblock micelles for drug delivery systems. These results represented that as a delivery platform, PLA–PEG–PLA nanoparticles could be able to boost the efficacy of Brevinin-2R cellular uptake. The Fig. 6A displays confocal optical images of the AGS, KYSE-30 and HepG2 cancer cells after 4 h incubation with PLA–PEG–PLA–FITC.

Loading Efficiency and In Vitro Drug Release

Mean Brevinin-2R entrapment efficiency from three independent assessments was approximately 95%. This could be due to intermolecular interactions. The in vitro release of Brevinin-2R from PLA–PEG–PLA micelles was investigated using the dialysis method in PBS (pH 7.4) as a release medium to simulate the physiological condition. Brevinin-2R is an amphiphilic peptide that can be dissolved in water. Thus, the release profile would be comparable with a hydrophilic drug such as 5-FU (Venkatraman et al. 2005). The Brevinin-2R-conjugated micelles showed a biphasic release profile (Fig. 6B); the vast majority of Brevinin-2Rs were released from Brevinin-2R-loaded micelles during transitional release in primary phase 2–8 days; after the primary stage, the release reached a plateau; for a small percentage of Brevinin-2R, release possibly has taken place in 12 days caused by the gradual degradation of copolymer and diffusion of Brevinin-2R entrapped inside the nanoparticles. The cumulative release of Brevinin-2R from sub layers of nanoparticles after 8 days was 88.5%; almost all the entrapped Brevinin-2R was released within 20 days in PBS medium. It was found that micelles indicated a superior drug release that is consistent with previous studies for 5-FU (Venkatraman et al. 2005). Copolymeric micelles, in part, prolonged release time and increased inhibitory effect of Brevinin-2R.

Based on former studies, PLA–PEG–PLA micelles are highly effective in encapsulation and the sustained release of therapeutic agents (Phan et al. 2016; Venkatraman et al. 2005).

Cell Viability Assay

In vitro cytotoxicity of blank nanoparticles, free Brevinin-2R and Brevinin-2R-conjugated PLA–PEG–PLA micelles was investigated on AGS, HepG2, KYSE-30 and HGF1-PI cells by MTT and NR methods in the range of concentrations tested using non-treated cells as the control. As shown in Fig. 7A, blank nanoparticles did not show any cytotoxic effect on treated cell lines, which indicated the biocompatibility of nanoparticles as the defining characteristics for a delivery system. On the other hand, both free Brevinin-2R and Brevinin-2R-conjugated micelles dramatically decreased cell viability of AGS, KYSE-30 and HepG2 cells in a time and dose-dependent trend. However, the sensitivity of the treated cells towards the cytotoxic effect of Brevinin-2R-loaded nanoparticles was more than that of Brevinin-2R, Fig. 7C–E. The IC_{50} values of the Brevinin-2R and Brevinin-2R-loaded nanoparticles have been shown in Table 1. These values highlighted that at the same time intervals, the Brevinin-2R-loaded nanoparticles had higher inhibitory effects on the mentioned cancer cell lines compared to the Brevinin-2R ($P < 0.05$), which can be attributed to the increased cellular uptake. Brevinin-2R-loaded micelles were efficiently internalized by the AGS, HepG2 and KYSE-30 cells. These results demonstrated that incorporation of Brevinin-2R into PLA–PEG–PLA micelles maintained the anti-proliferation effect of Brevinin-2R. The AGS cells showed higher sensitivity towards Brevinin-2R and Brevinin-2R-loaded copolymer than the two other cells. On the other hand, at the investigated concentrations, Brevinin-2R and Brevinin-2R-loaded nanoparticles showed negligible cytotoxic effects on HGF1-PI cell as a control non-tumor cell line Fig. 7B.

Cell Cycle Analysis

Cell cycle analysis detected intense Sub G1 arrest in Brevinin-2R and Brevinin-2R-loaded nanoparticles treated AGS, HepG2 and KYSE-30 cells compared to untreated
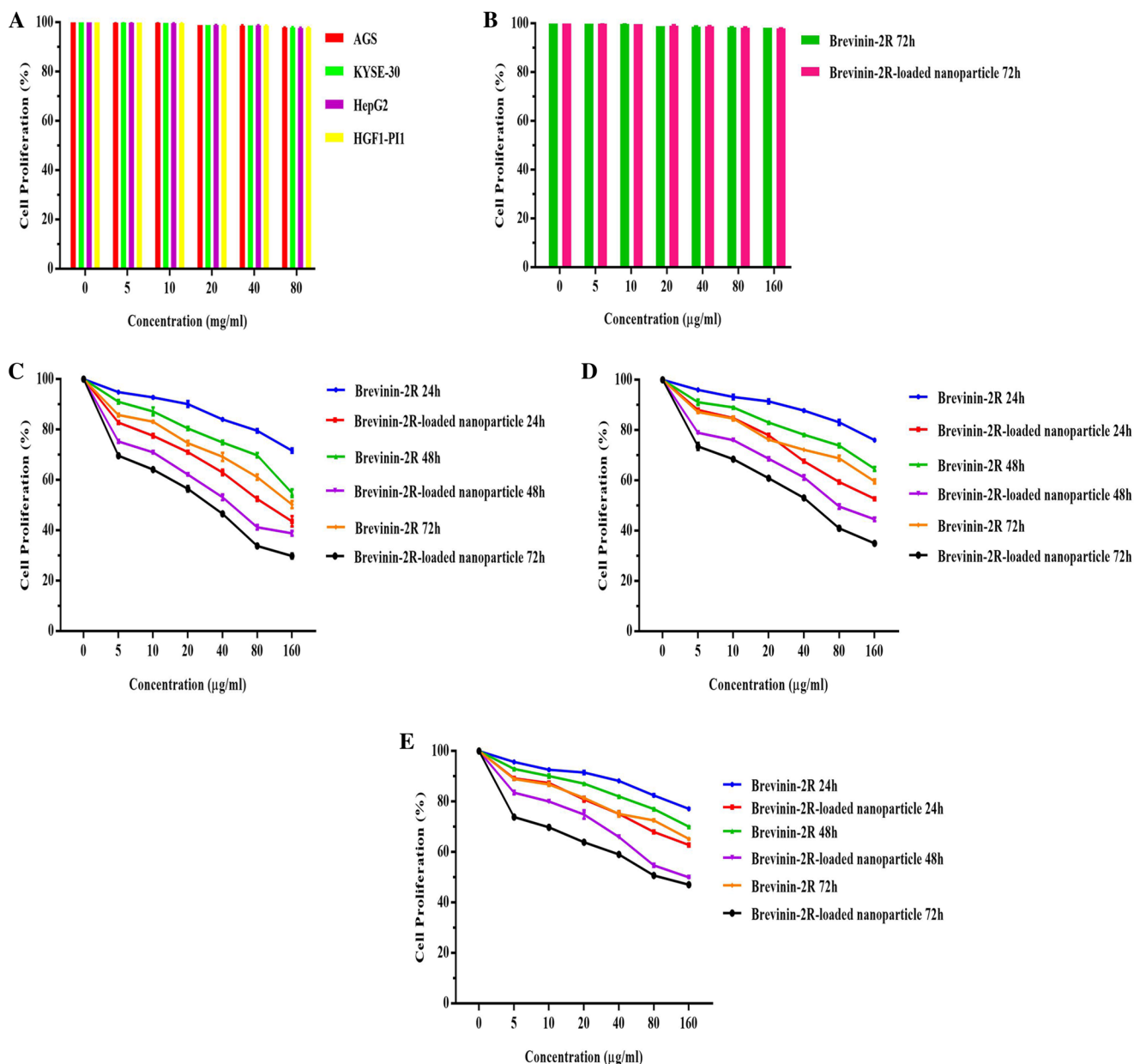
Fig. 7 A Viability test for treated AGS, KYSE-30, HepG2 and HGF1-PI1 cell lines with PLA–PEG–PLA nanoparticles measured by MTT assay; viability study of treated **B** HGF1-PI, **C** AGS, **D** HepG2 and **E** KYSE-30 cell lines with Brevinin-2R and Brevinin-2R-loaded micelles at different concentrations measured through MTT, after 24, 48, and 72 h; each point represents mean ± SD, and error bars represent the SD (n = 3). The differences in cytotoxicity between free Brevinin-2R and Brevinin-2R-conjugated micelles are significant (P < 0.05)

Table 1 The average IC_{50} values for (a) Brevinin-2R, (b) Brevinin-2R-loaded nanoparticles for treated AGS, HepG2 and KYSE-30 cell lines after 24, 48, and 72 h measured through MTT and neutral red uptake assays; data are as mean $\pm$ SD (n = 3), P < 0.0 5

Cell line (time)	IC_{50} by MTT assay (µg/ml)	IC_{50} by neutral red assay (µg/ml)	Total IC_{50} (µg/ml)
(a)			
AGS 24 h	279.81 ± 7.9	285.29 ± 2.7	282.55 ± 5.3
AGS 48 h	167.78 ± 6.4	157.71 ± 4.2	162.74 ± 5.3
AGS 72 h	141.58 ± 1.8	140.06 ± 1.6	140.82 ± 1.7
HepG2 24 h	340.65 ± 1.2	334.41 ± 1.8	337.53 ± 1.5
HepG2 48 h	221.35 ± 5.3	215.36 ± 1.4	218.35 ± 3.3
HepG2 72 h	188.45 ± 5.1	186.25 ± 3.5	187.35 ± 4.3
KYSE-30 24 h	356.78 ± 4.7	358.48 ± 2.9	357.63 ± 3.8
KYSE-30 48 h	266.33 ± 1.4	265.45 ± 4.5	265.89 ± 2.9
KYSE-30 72 h	225.52 ± 2	221.4 ± 4.2	223.46 ± 3.1
(b)			
AGS 24 h	114.44 ± 5	105.17 ± 5.1	109.80 ± 5
AGS 48 h	89.21 ± 2.6	79.23 ± 4	84.22 ± 3.3
AGS 72 h	66.84 ± 2.2	61.48 ± 1	64.16 ± 1.6
HepG2 24 h	145.12 ± 0.7	142.5 ± 3	143.81 ± 1.8
HepG2 48 h	112.03 ± 1.04	107.03 ± 2.6	109.53 ± 1.8
HepG2 72 h	82.76 ± 0.6	81.03 ± 1.4	81.89 ± 1
KYSE-30 24 h	199.75 ± 3.3	197.74 ± 3.7	198.74 ± 3.5
KYSE-30 48 h	132.55 ± 1.4	129.13 ± 2.8	130.84 ± 2.1
KYSE-30 72 h	115.76 ± 1.6	109.19 ± 1.8	112.47 ± 1.7

control cells. Also, the percentages of cells in G2-M phase dropped remarkably after 48 h of treatment. In comparison with Brevinin-2R treated cells, higher percentages of cell arrest were observed in cancer cells treated with Brevinin-2R-conjugated nanoparticles. In AGS cell line, treated with Brevinin-2R and Brevinin-2R-loaded nanoparticles compared to untreated control cells, 22.58% and 48.77% of cells were arrested in Sub G1 phase, respectively (Fig. 8). After 48 h of incubation, up to 18.70% and 43.30% of HepG2 cells treated with Brevinin-2R and Brevinin-2R-loaded

nanoparticles were captured in Sub G1 stage of the cell cycle and KYSE-30 rates were 13.30% and 38.21%, respectively (P < 0.05).

Apoptosis Study

Brevinin-2R induced apoptosis cascade in cancer cells. Compared to Brevinin-2R treated cells, the higher rates of apoptosis were witnessed in cells treated with Brevinin-2R-conjugated nanoparticles (Fig. 9). Regarding AGS, compared to the control, 16.44% and 27.66% of cells under treatment with Brevinin-2R and Brevinin-2R-conjugated nanoparticles undertook apoptosis, respectively. In the interim, 13.99% and 25.03% of HepG2 cells saw apoptosis in treated cells with Brevinin-2R and Brevinin-2R-conjugated nanoparticles. In comparison to 12.58% apoptotic cells in KYSE-30 treated with Brevinin-2R, 21.55% of cells were captured by apoptosis in treated cells with Brevinin-2R-conjugated nanoparticles (P < 0.05).

Conclusions

There has been an increasing interest in the usage of broad-spectrum, alternative natural anticancer agents, such as drug peptides to address the problems related to cancer therapy. Our findings showed that the synthesized PLA–PEG–PLA copolymeric micelles, as biocompatible carriers, increased the inhibitory effect of Brevinin-2R on AGS, HepG2 and KYSE-30 cells. Furthermore, this nanoparticle caused higher cell cycle arrest and apoptosis induced by Brevinin-2R-conjugated nanoparticles compared to that of Brevinin-2R. In conclusion, through protection from proteolytic decomposition and sustained release behavior, leading to improved anticancer activity (Zhang et al. 2017), PLA–PEG–PLA triblock copolymer can act as a promising nano drug delivery system for hydrophilic therapeutic agents such as Brevinin-2R. This is the first study on the anti-proliferative effect of Brevinin-2R and Brevinin-2R incorporated into PLA–PEG–PLA on gastric, hepatocellular and squamous
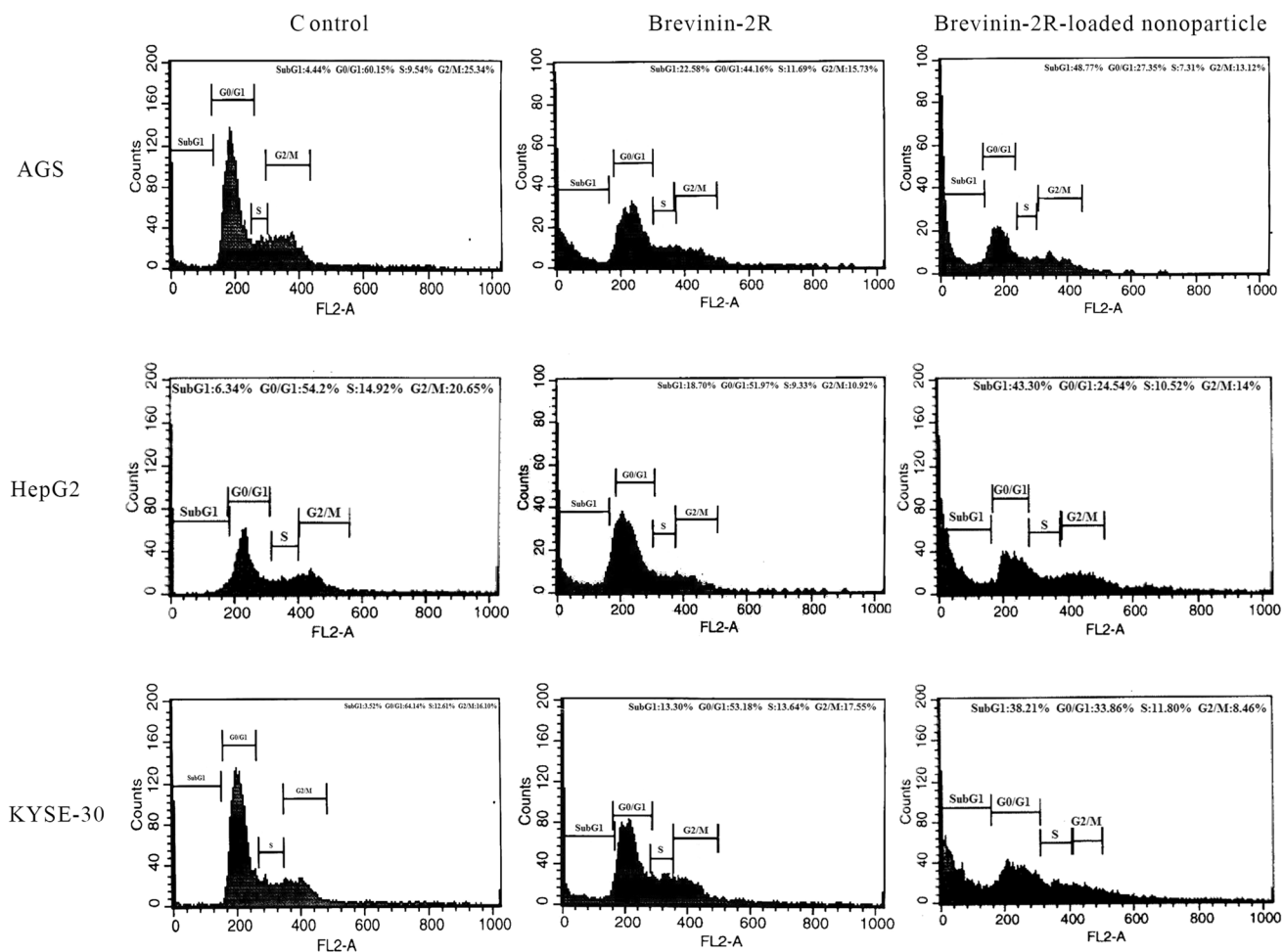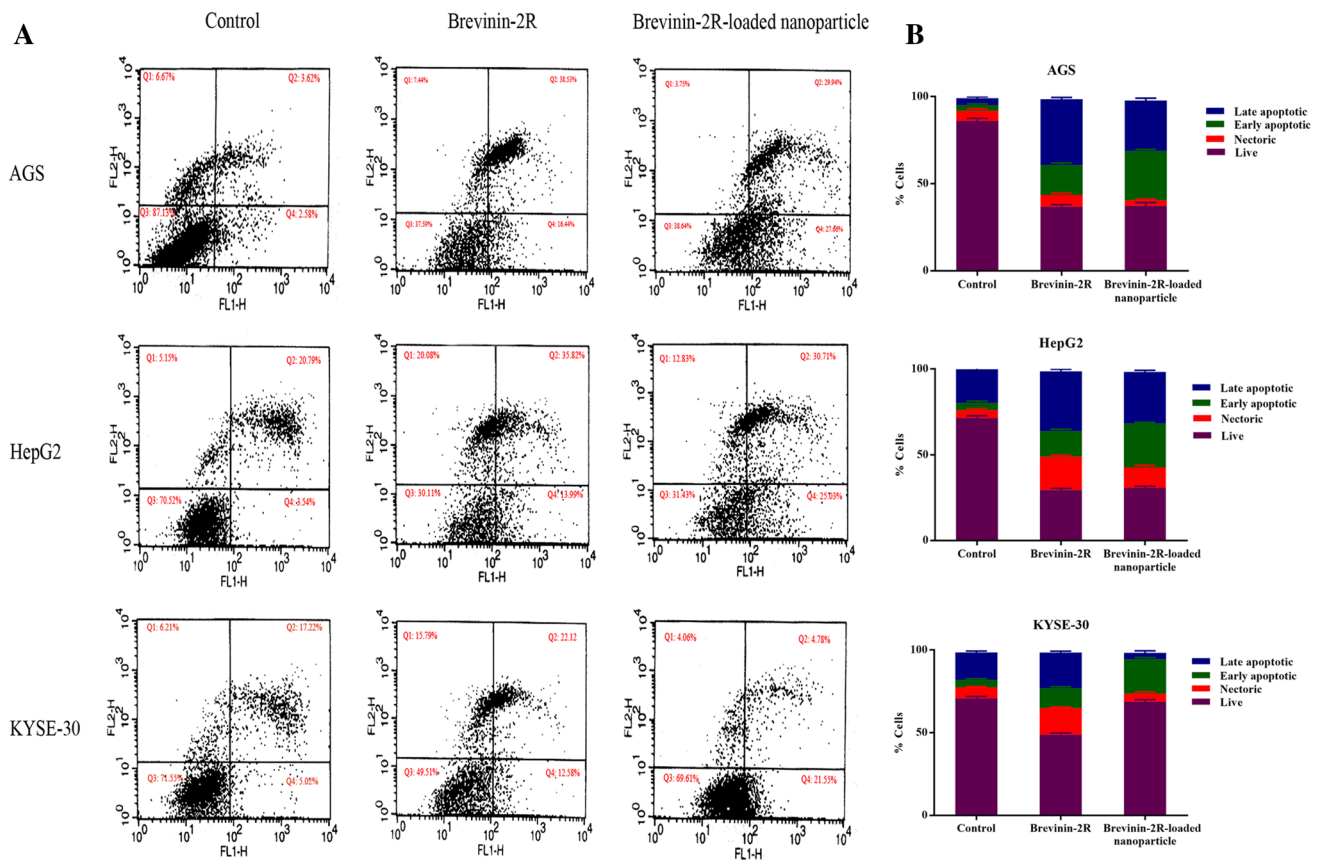
Fig. 8 After 48 h treatment with IC_{50} concentrations of Brevinin-2R and Brevinin-2R conjugated PLA–PEG–PLA, cell cycle distributions were analyzed by flow cytometry. Each value is a representative of three independent experiments compared to the untreated same cells. Data are as mean $\pm$ SD, $P < 0.05$. In comparison with Brevinin-2R, Brevinin-2R-loaded nanoparticles induced higher rates of Sub G1 Cell cycle arrest in treated cells

carcinoma cells. With reduced IC_{50} values, when conjugated with PLA–PEG–PLA nanoparticle as a biocompatible delivery system, Brevinin-2R could be an alternative anti-cancer therapeutic agent in lieu of chemotherapy and its side effects. Additional studies will be required to examine the possibilities of this potential delivery system in vivo.

Fig. 9 A The effects of the Brevinin-2R and Brevinin-2R-conjugated PLA–PEG–PLA on apoptosis induction in AGS, HepG2 and KYSE-30 cell lines after 48 h treatment with IC_{50} concentrations for each cell line were determined by AV/PI staining. Samples were analyzed using a flow cytometry and representative dot plot is illustrated. Q1: necrotic, AV −/PI+; Q2: late apoptotic, AV +/PI+; Q3: live, AV −/ PI −; Q4: early apoptotic, AV + /PI −; the graphs are representative of three independent experiments compared to untreated control cells. Data are as mean ± SD, P < 0.05. Compared to Brevinin-2R, Brevinin-2R-loaded nanoparticles induced higher rates of apoptosis in treated cells. **B** Bar diagrams of cells which are positive for annexin-V, PI and both annexin-V/PI

Compliance with Ethical Standards

Conflict of interest The authors declare that they have no conflict of interest.

Research Involving Human and Animal Participants This article does not contain any studies with human participants or animals performed by any of the authors.

Informed Consent Informed consent was obtained from all individual participants included in the study.

References

Allum W, Lordick F, Alsina M, Andritsch E, Ba-Ssalamah A, Beishon M, Braga M, Caballero C, Carneiro F, Cassinello F, Dekker JW (2018) ECCO essential requirements for quality cancer care: oesophageal and gastric cancer. Crit Rev Oncol Hematol 122:179–193. https://doi.org/10.1016/j.critrevonc.2017.12.019

Amaral AC, Silva ON, Mundim NC, de Carvalho MJ, Migliolo L, Leite JR, Prates MV, Bocca AL, Franco OL, Felipe MS (2012) Predicting antimicrobial peptides from eukaryotic genomes: in silico strategies to develop antibiotics. Peptides 37:301–308. https://doi.org/10.1016/j.peptides.2012.07.021

Asadi H, Rostamizadeh K, Salari D, Hamidi M (2011) Preparation of biodegradable nanoparticles of tri-block PLA–PEG–PLA copolymer and determination of factors controlling the particle size using artificial neural network. J Microencapsul 28:406–416. https://doi.org/10.3109/02652048.2011.576784

Asoodeh A, Haghparast A, Kashef R, Chamani J (2013) Pro-inflammatory cytokine responses of A549 epithelial cells to antimicrobial peptide Brevinin-2R. Int J Pept Res Ther 19:157–162. https://doi.org/10.1007/s10989-012-9328-6

Chan JM, Zhang L, Yuet KP, Liao G, Rhee JW, Langer R, Farokhzad OC (2009) PLGA lecithin–PEG core shell nanoparticles for controlled drug delivery. Biomaterials 30:1627–1634. https://doi.org/10.1016/j.biomaterials.2008.12.013

Chau Y, Padera RF, Dang NM, Langer R (2006) Antitumor efficacy of a novel polymer-peptide-drug conjugate in human tumor xenograft models. Int J Cancer 118:1519–1526. https://doi.org/10.1002/ijc.21495

Davies EA, Bevis HE, Delves-Broughton J (1997) The use of the bacteriocin, nisin, as a preservative in ricotta type cheeses to control the food-borne pathogen *Listeria monocytogenes*. Lett Appl Microbiol 24(5):343–346. https://doi.org/10.1046/j.1472-765X.1997.00145.x

Dell'Erba R, Groeninckx G, Maglio G, Malinconico M, Migliozzi A (2001) Immiscible polymer blends of semicrystalline biocompatible components: thermal properties and phase morphology analysis of PLLA/PCL blends. Polymer 42:7831–7840. https://doi.org/10.1016/S0032-3861(01)00269-5

Duda A, Biela T, Libiszowski J, Penczek S, Dubois P, Mecerreyes D, Jérôme R (1998) Block and random copolymers of ε-caprolactone. Polym Degrad Stab 59:215–222. https://doi.org/10.1016/S0141-3910(97)00167-5

Ghavami S, Asoodeh A, Klonisch T, Halayko AJ, Kadkhoda K, Kroczak TJ, Gibson SB, Booy EP, Naderi-Manesh H, Los M (2008) Brevinin-2R[1] semi-selectively kills cancer cells by a distinct mechanism, which involves the lysosomal-mitochondrial death pathway. J Cell Mol Med 12:1005–1022. https://doi.org/10.1111/j.1582-4934.2008.00129.x

Ghodsi-Moghadam B, Asoodeh A (2018) The impact of Brevinin-2R peptide on oxidative statues and antioxidant enzymes in human epithelial cell line of A549. Int J Pept Res Ther. https://doi.org/10.1007/s10989-018-9754-1

Hami Z, Amini M, Ghazi-Khansari M, Rezayat SM, Gilani K (2014a) Doxorubicin conjugated PLA-PEG-Folate based polymeric micelle for tumor-targeted delivery: synthesis and in vitro evaluation. Daru J Pharm Sci 22:30. https://doi.org/10.1186/2008-2231-22-30

Hami Z, Amini M, Ghazi-Khansari M, Rezayat SM, Gilani K (2014b) Synthesis and in vitro evaluation of a pH sensitive PLA–PEG–folate based polymeric micelle for controlled delivery of docetaxel. Colloid Surface B 116:309–317. https://doi.org/10.1016/j.colsurfb.2014.01.015

He G, Ma LLL, Pan J, Venkatraman S (2007) ABA and BAB type triblock copolymers of PEG and PLA: a comparative study of drug release properties and "stealth" particle characteristics. Int J Pharm 334:48–55. https://doi.org/10.1016/j.ijpharm.2006.10.020

Hilpert K, Fjell CD, Cherkasov A (2008) Short linear cationic antimicrobial peptides: screening, optimizing, and prediction. Methods Mol Biol 494:127–159. https://doi.org/10.1007/978-1-59745-419-3_8

Hobbs SK, Monsky WL, Yuan F, Roberts WG, Griffith L, Torchilin VP, Jain RK (1998) Regulation of transport pathways in tumor vessels: role of tumor type and microenvironment. Proc Natl Acad Sci 95:4607–4612. https://doi.org/10.1073/pnas.95.8.4607

Homayouni-Tabrizi M, Asoodeh A, Soltani M, Forghanifard MM (2015) Antimicrobial peptide Brevinin-2R induces the secretion of a pro-inflammatory cytokine in HepG2 cells. J Basic Res Med Sci 2:23–29

Hrubý M, Koňák Č, Ulbrich K (2005) Polymeric micellar pH-sensitive drug delivery system for doxorubicin. J Control Release 103:137–148. https://doi.org/10.1016/j.jconrel.2004.11.017

Jelonek K, Li S, Kaczmarczyk B, Marcinkowski A, Orchel A, Musiał-Kulik M, Kasperczyk J (2016) Multidrug PLA-PEG filomicelles for concurrent delivery of anticancer drugs—the influence of drug-drug and drug polymer interactions on drug loading and release properties. Int J Pharm 510:365–374. https://doi.org/10.1016/j.ijpharm.2016.06.051

Jemal A, Bray F, Center MM, Ferlay J, Ward E, Forman D (2011) Global cancer statistics. CA Cancer J Clin 61:69–90. https://doi.org/10.3322/caac.20107

Kakde D, Jain D, Shrivastava V, Kakde R, Patil AT (2011) Cancer therapeutics-opportunities, challenges and advances in drug delivery. J Appl Pharm Sci 1:1–10

Kataoka K, Harada A, Nagasaki Y (2001) Block copolymer micelles for drug delivery: design, characterization and biological significance. Adv Drug Deliv Rev 47:113–131. https://doi.org/10.1016/j.addr.2012.09.013

Li W, Gao YQ (2018) MiR-217 is involved in the carcinogenesis of gastric cancer by down-regulating CDH1 expression. Kaohsiung J Med Sci. https://doi.org/10.1016/j.kjms.2018.02.003

Li P, Dai YN, Zhang JP, Wang AQ, Wei Q (2008) Chitosan-alginate nanoparticles as a novel drug delivery system for nifedipine. Int J Biomed Sci 4:221–228

Licciardi M, Cavallaro G, Di Stefano M, Pitarresi G, Fiorica C, Giammona G (2010) New self-assembling polyaspartylhydrazide copolymer micelles for anticancer drug delivery. Int J Pharm 396:219–228. https://doi.org/10.1016/j.ijpharm.2010.06.021

Massodi I, Moktan S, Rawat A, Bidwell GL, Raucher D (2010) Inhibition of ovarian cancer cell proliferation by a cell cycle inhibitory peptide fused to a thermally responsive polypeptide carrier. Int J Cancer 126:533–544. https://doi.org/10.1002/ijc.24725

Mehrnejad F, Naderi-Manesh H, Ranjbar B, Maroufi B, Asoodeh A, Doustdar F (2008) PCR-based gene synthesis, molecular cloning, high level expression, purification, and characterization of novel antimicrobial peptide, brevinin-2R, in *Escherichia coli*. Appl Biochem Biotechnol 149:109–118. https://doi.org/10.1007/s12010-007-8024-z

Middleton DR, Bouaoun L, Hanisch R, Bray F, Dzamalala C, Chasimpha S, Menya D, Mbalawa CG, N'Da G, Woldegeorgis MA, Njie R (2018) Esophageal cancer male to female incidence ratios in Africa: a systematic review and meta-analysis of geographic, time and age trends. Cancer Epidemiol 53:119–128. https://doi.org/10.1016/j.canep.2018.01.020

Nakagawa H, Fujita M, Fujimoto A (2018) Genome sequencing analysis of liver cancer for precision medicine. Semin Cancer Biol. https://doi.org/10.1016/j.semcancer.2018.03.004

Perez-Tomas R (2006) Multidrug resistance: retrospect and prospects in anti-cancer drug treatment. Curr Med Chem 13:1859–1876. https://doi.org/10.2174/092986706777585077

Phan QT, Le MH, Le TT, Tran TH, Xuan PN, Ha PT (2016) Characteristics and cytotoxicity of folate-modified curcumin-loaded PLA-PEG micellar nano systems with various PLA:PEG ratios. Int J Pharm 507:32–40. https://doi.org/10.1016/j.ijpharm.2016.05.003

Venkatraman SS, Jie P, Min F, Freddy BY, Leong-Huat G (2005) Micelle-like nanoparticles of PLA-PEG-PLA triblock copolymer as chemotherapeutic carrier. Int J Pharm 298:219–232. https://doi.org/10.1016/j.ijpharm.2005.03.023

Wolinsky JB, Colson YL, Grinstaff MW (2012) Local drug delivery strategies for cancer treatment: gels, nanoparticles, polymeric films, rods, and wafers. J Control Release 159:14–26. https://doi.org/10.1016/j.jconrel.2011.11.031

Woraphatphadung T, Sajomsang W, Rojanarata T, Ngawhirunpat T, Tonglairoum P, Opanasopit P (2018) Development of chitosan-based pH-sensitive polymeric micelles containing curcumin for colon targeted drug delivery. AAPS PharmSciTech 19:991–1000. https://doi.org/10.1208/s12249-017-0906-y

Xiao RZ, Zeng ZW, Zhou GL, Wang JJ, Li FZ, Wang AM (2010) Recent advances in PEG-PLA block copolymer nanoparticles. Int J Nanomed 5:1057–1065. https://doi.org/10.2147/IJN.S14912

Yokoyama M (2011) Clinical applications of polymeric micelle carrier systems in chemotherapy and image diagnosis of solid

tumors. J Exp Clin Med 3:151–158. https://doi.org/10.1016/j.jecm.2011.06.002

Zhang Y, Ren T, Gou J, Zhang L, Tao X, Tian B, Tian P, Yu D, Song J, Liu X, Chao Y (2017) Strategies for improving the payload of small molecular drugs in polymeric micelles. J Control Release 261:352–366. https://doi.org/10.1016/j.jconrel.2017.01.047

Zhao H, Liu Z, Park SH, Kim SH, Kim JH, Piao L (2012) Preparation and characterization of PEG/PLA multiblock and triblock copolymer. Bull Korean Chem Soc 33:1638–1642. https://doi.org/10.5012/bkcs.2012.33.5.1638

Zohri M, Alavidjeh MS, Haririan I, Ardestani MS, Ebrahimi SE, Sani HT, Sadjadi SK (2010) A comparative study between the antibacterial effect of nisin and nisin-loaded chitosan/alginate nanoparticles on the growth of *Staphylococcus aureus* in raw and pasteurized milk samples. Probiotics Antimicrob Proteins 2(4):258–266. https://doi.org/10.1007/s12602-010-9047-2